Photochemistry and Photobiology, 2013, 89: 68–73

Structure-Dependent Demetalation Kinetics of Chlorophyll *a* Analogs under Acidic Conditions

Yoshitaka Saga*[1], Yuki Hirai[1], Kana Sadaoka[1], Megumi Isaji[2] and Hitoshi Tamiaki[2]

[1]Department of Chemistry, Faculty of Science and Engineering, Kinki University, Higashi-Osaka, Osaka, Japan
[2]Department of Bioscience and Biotechnology, Faculty of Science and Engineering, Ritsumeikan University, Kusatsu, Shiga, Japan

Received 22 May 2012, accepted 19 July 2012, DOI: 10.1111/j.1751-1097.2012.01213.x

ABSTRACT

Demetalation of chlorophyll (Chl) *a* and its analogs is an important reaction in oxygenic photosynthetic organisms, which produces the primary electron acceptors in photosystem II reaction centers and is crucial in the Chl degradation. From these viewpoints, demetalation reactions of four Chl *a* analogs, 3,8-divinyl-Chl *a* (DV-Chl *a*), 3-devinyl-3-ethyl-Chl *a* (mesoChl *a*), 13^2-demethoxycarbonyl-Chl *a* (pyroChl *a*) and protochlorophyll *a* (PChl *a*), were kinetically analyzed under weakly acidic conditions, and were compared with that of Chl *a*. DV-Chl *a* exhibited slower demetalation kinetics than did Chl *a*, whereas demetalation of mesoChl *a* was faster than that of Chl *a*. The difference in demetalation kinetics of the three chlorophyllous pigments originates from the electron-withdrawing ability of the vinyl group as the peripheral substituent compared with the ethyl group. Removal of the electron-withdrawing and homoconjugating 13^2-methoxycarbonyl group in Chl *a* (Chl *a* → pyroChl *a*) accelerated demetalation kinetics by two-fold. PChl *a* possessing the porphyrin-type skeleton exhibited slower demetalation kinetics than Chl *a*. The structure-dependent demetalation properties of Chl *a* analogs will be useful for understanding *in vivo* Chl demetalation reactions in oxygenic photosynthetic organisms.

INTRODUCTION

Chlorophyll (Chl) *a* is the most abundant photosynthetic pigment in nature, and plays important roles in photosynthetic activities, such as photoinduced charge separation, electron transfer and excitation energy transfer in oxygenic photosynthetic organisms (1). Figure 1 shows the molecular structure of Chl *a*. Chl *a* has a central magnesium in the chlorin macrocycle, which is a 17,18-dihydroporphyrin, with an isocyclic five-membered ring. The saturation of the C17–C18 bond in the D-ring of Chl *a* is responsible for its spectral properties, which are appropriate for efficient light-harvesting and energy transduction during photosynthesis.

Naturally occurring Chls in oxygenic photosynthetic organisms are commonly monovinyl pigments in terms of the peripheral substituents (1,2). The exceptions are divinyl (DV) pigments (3,8-divinyl-Chls (DV-Chls) *a* and *b* as well as Chls c_2 and c_3) and Chl *d* that has no vinyl group (1–7). Marine cyanobacteria, *Prochlorococcus* species, possess DV-Chls *a* and *b* as major pigments (3–5). The molecular structure of DV-Chl *a* is depicted in Fig. 1. DV-Chl *a* has a vinyl group at the 8-position, whereas this position is substituted by an ethyl group in Chl *a*. Owing to the 8-vinyl group, the Soret absorption bands of DV-Chls are redshifted by *ca* 10 nm relative to the corresponding 3-vinyl-8-ethyl-Chls. Such spectral properties would be advantageous for efficient absorption of blue light by *Prochlorococcus* species.

Oxygenic photosynthetic organisms have two types of reaction centers, namely photosystem (PS) I and PS II. A demetalation product of Chl *a*, namely pheophytin (Phe) *a*, functions as the primary electron acceptor in PS II of most oxygenic photosynthetic organisms (8–11). In contrast, a mutant of *Synechocystis* sp. PCC6803, which is not able to hydrogenate the 8-vinyl group and accumulate DV-Chl *a*, was reported to possess DV-Phe *a* as the primary electron acceptor in PS II, instead of Phe *a* (12). Biosynthesis of Phe *a* and DV-Phe *a* as the key cofactors of PS II remains completely unknown in spite of its biological importance. Chl *a* and DV-Chl *a* would be the precursors of Phe *a* and DV-Phe *a*, respectively, in PS II, as Chl synthases use chlorophyllide (Chlide) *a* and DV-Chlide *a* as substrates to esterify a long hydrocarbon chain at the 17-propionate and cannot use pheophorbide (Pheide) *a* lacking the central metal (13,14). Therefore, demetalation of Chl *a* and DV-Chl *a* is a key reaction in the biosynthesis of Phe molecules that function as the primary electron acceptors in PS II.

Demetalation of chlorophyllous pigments is also crucial in the Chl degradation pathway (15–18). Chl degradation is one of the most large-scale bioprocesses on earth and a major origin of beautiful color changes of plant leaves in autumn. The first step in Chl *a* degradation would be removal of the central magnesium. The resulting Phe *a* is converted to Pheide *a* by hydrolysis of the phytyl ester by pheophytinase (19,20). From this point of view, demetalation properties of Chl *a* and its analogs have attracted considerable attention as well.

Physicochemical studies of demetalation properties of chlorophyllous pigments will provide useful information to unravel biologically important reactions in photosynthetic organisms described above, and *in vitro* demetalation of natural Chls and their model compounds have been examined (21–35). Mackinney and Joslyn first reported difference in demetalation kinetics between Chls *a* and *b* in the early 1940s (21,22). Watanabe *et al.* examined detailed demetalation properties of Chls *a*, *b* and their epimers (Chls *a*′ and *b*′, respectively; 26,27). Kobayashi *et al.* analyzed demetalation of zinc bacteriochlorophyll (BChl) *a* (28), which was discovered in a purple photosynthetic bacterium,

*Corresponding author email: saga@chem.kindai.ac.jp (Yoshitaka Saga)
© 2012 Wiley Periodicals, Inc.
Photochemistry and Photobiology © 2012 The American Society of Photobiology 0031-8655/13

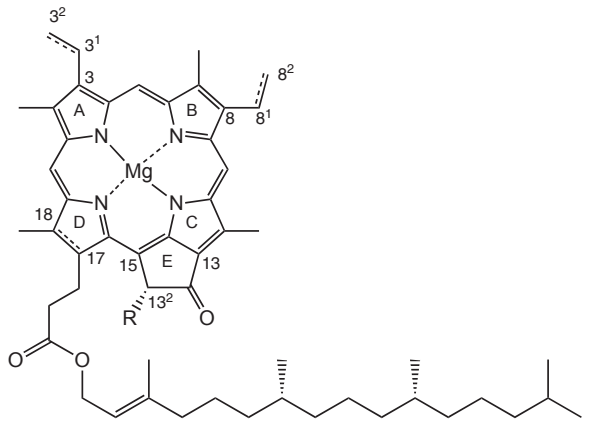

	$C3^1$–$C3^2$	$C8^1$–$C8^2$	C17–C18	R
Chl *a*	double bond	single bond	single bond	$COOCH_3$
DV-Chl *a*	double bond	double bond	single bond	$COOCH_3$
mesoChl *a*	single bond	single bond	single bond	$COOCH_3$
pyroChl *a*	double bond	single bond	single bond	H
PChl *a*	double bond	single bond	double bond	$COOCH_3$

Figure 1. Molecular structures of Chl *a*, DV-Chl *a*, mesoChl *a*, pyroChl *a* and PChl *a*.

Acidiphilium rubrum (36,37). Recently, we examined demetalation properties of other naturally occurring (B)Chls (29–31) and synthetic zinc complexes (32–35), which were model compounds of natural Chls. These studies indicate that peripheral substituents on the chlorin macrocycle are responsible for physicochemical properties on demetalation of chlorophyllous pigments. However, there are few studies on demetalation of Chl *a* analogs concerning important metabolic intermediates. In addition, no information is available, to our best knowledge, on demetalation of DV-Chl *a*, which is a major photosynthetic pigment and would be a precursor of the primary electron acceptor in PS II in a Δslr1923 mutant of *Synechocystis* sp. PCC6803. Herein, we report demetalation properties of four Chl *a* analogs, DV-Chl *a*, 3-devinyl-3-ethyl-Chl *a* (mesoChl *a*), 13^2-demethoxycarbonyl-Chl *a* (pyroChl *a*) and protochlorophyll *a* (PChl *a*). Figure 1 shows molecular structures of the four Chl *a* analogs used in this study. DV-Chl *a* possesses two vinyl groups at the 3- and 8-positions, whereas ethyl groups occupy both the positions in mesoChl *a*. Comparison of demetalation properties among these two Chl *a* analogs as well as intact Chl *a* enables us to elucidate the substitution effects in the A- and B-rings of Chl *a*. pyroChl *a* lacks a methoxycarbonyl group at the 13^2-position, and is a good pigment to investigate the effect of the 13^2-methoxycarbonyl group in Chl *a* on demetalation. PChl *a* has the porphyrin-type macrocycle as the functional moiety and is an analog of the important intermediates, protochlorophyllide (PChlide) *a*, in the Chl *a* biosynthesis. Demetalation kinetics of PChl *a*, in which only the bond between C17 and C18 atoms differs from that in Chl *a*, allows us to understand how macrocyclic structures of magnesium cyclic tetrapyrroles affect their demetalation properties.

MATERIALS AND METHODS

Apparatus. Visible absorption spectra were measured using a Shimadzu UV-2450 spectrophotometer (Shimadzu, Ltd., Kyoto, Japan), where the reaction temperature was regulated with a Shimadzu thermo-electric temperature-controlled cell holder TCC-240A. High-performance liquid chromatography (HPLC) was performed with a Shimadzu LC-20AT pump and an SPD-M20A or SPD-20AV detector.

Materials. DV-Chl *a* and Chl *a* were isolated from a Δslr1923 mutant of *Synechocystis* sp. PCC6803 and *Spirulina geitleri*, respectively (38,39). Three other chlorophyllous pigments, mesoChl *a*, pyroChl *a* and PChl *a*, were synthesized from Chl *a* according to previous reports (38–40). The 3-vinyl group of Chl *a* was hydrogenated in the presence of palladium charcoal under hydrogen atmosphere to give mesoChl *a* (39). Pyrolysis of Chl *a* in γ-collidine provided pyroChl *a* lacking the 13^2-methyoxycarbonyl group (40). PChl *a* was obtained by oxidation of Chl *a* with 2,3-dichloro-5,6-dicyano-1,4-benzoquinone (38,39). The four pigments were purified by reverse-phase HPLC just before measurements of demetalation kinetics.

Measurements of demetalation kinetics. A 3.0 mL acetone solution of purified chlorophyllous pigments (Soret absorbance = 1.0 at the 1 cm pathlength) was mixed with 1.0 mL of distilled water. A 10 μL of aqueous hydrochloric acid for volumetric analysis (Wako Pure Chemical Industries, Ltd., Osaka, Japan) was added to the solutions, and absorbance at the Soret peak positions of chlorophyllous pigments was followed in time under the control of reaction temperatures at 25°C. The proton concentrations were estimated by assumption of complete dissociation of hydrochloric acid in a mixture of acetone and water (3/1, vol/vol), as was ensured in the cases of proton concentrations below 10^{-1} M in previous reports (26,28).

Pigment analysis after demetalation. After demetalation reactions of DV-Chl *a*, mesoChl *a* and pyroChl *a*, the solutions were neutralized with aqueous 4% $NaHCO_3$, and the pigments were extracted with CH_2Cl_2. The CH_2Cl_2 solutions were washed with aqueous saturated NaCl, and dried over anhydrous Na_2SO_4. The solutions were filtered and dried with nitrogen gas. In the case of demetalation of PChl *a*, the solutions after reactions were directly analyzed to avoid degradation of products through the extraction processes. The residues were analyzed on a reverse-phase HPLC column $5C_{18}$-AR-II (6 mmφ × 250 mm) with a guard column $5C_{18}$-AR-II (4.6 mmφ × 10 mm) with methanol/acetone (85/15, vol/vol) or a normal-phase column 5SL-II (6 mmφ × 250 mm) with hexane/2-propanol (99/1, vol/vol) at a flow rate of 1.0 mL min^{-1}.

RESULTS AND DISCUSSION

Spectral changes

Figure 2 depicts spectral changes in DV-Chl *a*, mesoChl *a*, pyroChl *a* and PChl *a* in aqueous acetone (acetone/water = 3/1, vol/vol) at 25°C. The 440-nm Soret absorption band of DV-Chl *a* gradually decreased and a new absorption band appeared at 419 nm under the present conditions, as shown in Fig. 2A. The 419-nm band was ascribed to the Soret band of the free-base of DV-Chl *a*, namely DV-Phe *a*. The Q_y absorbance at 665 nm of DV-Chl *a* also decreased by incubation in the acidic aqueous acetone. The isosbestic points were present at 429, 466 and 561 nm in this spectral change.

The other three Chl *a* analogs exhibited essentially the same spectral changes under the acidic conditions. The Soret and Q_y absorption bands at 427 and 652 nm, respectively, of mesoChl *a* decreased, accompanying increase in the 406-nm Soret band of mesoPhe *a* (Fig. 2B). The isosbestic points could be observed at 415, 450 and 554 nm. In the case of pyroChl *a*, 433-nm Soret and 664-nm Q_y absorbance became small with appearance of the 411-nm Soret band, which was derived from the production of pyroPhe *a* (Fig. 2C). This spectral change had the isosbestic points at 421, 457 and 557 nm. PChl *a* showed disappearance of the 435-nm Soret band and appearance of the 418-nm band, which was the Soret band of the pheophytinized PChl *a*, namely PPhe *a* (Fig. 2D). The small bands in the wavelength range between 500 and 700 nm gradually changed with several isosbestic points through demetalation of PChl *a* under the acidic conditions.

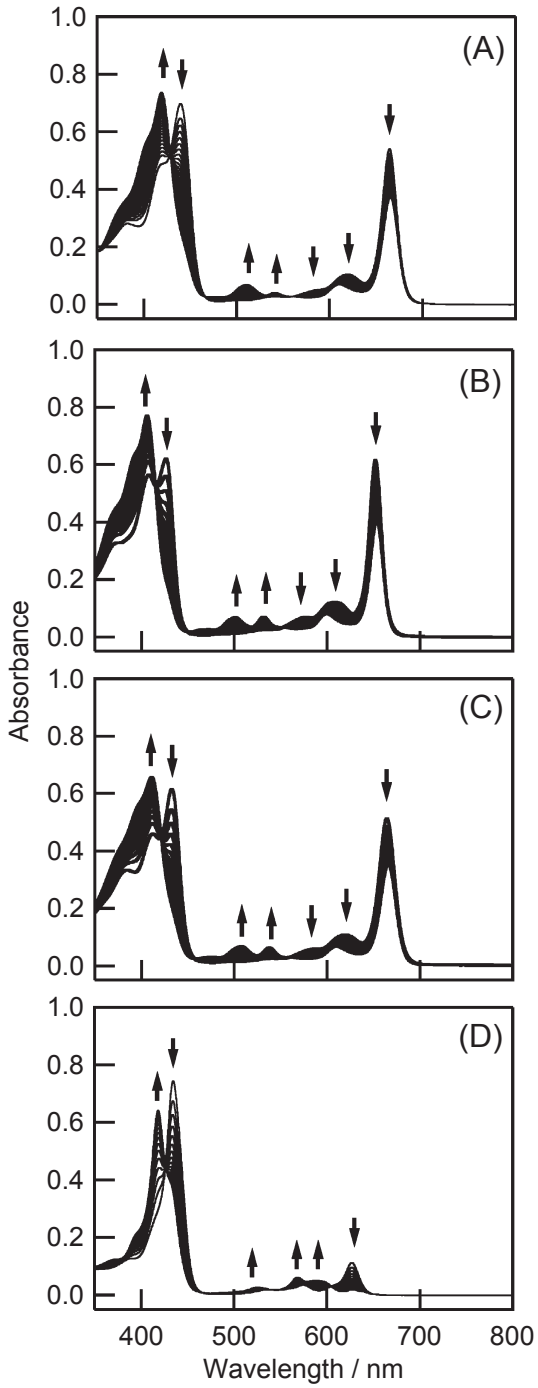

Figure 2. Spectral changes of DV-Chl *a* (A), mesoChl *a* (B), pyroChl *a* (C) and PChl *a* (D) in acetone/water (3/1, vol/vol). DV-Chl *a*: spectra from 0 to 150 min at 10-min intervals at the proton concentration of 2.5×10^{-4} M. mesoChl *a*: spectra from 0 to 150 min at 10-min intervals at the proton concentration of 1.2×10^{-4} M. pyroChl *a*: spectra from 0 to 150 min at 10-min intervals at the proton concentration of 1.2×10^{-4} M. PChl *a*: spectra from 0 to 450 min at 30-min intervals at the proton concentration of 2.5×10^{-4} M. The arrows show the direction of the absorbance changes.

Demetalation kinetics

Demetalation reactions of four Chl *a* analogs were quantitatively analyzed by monitoring absorbance changes at their Soret peak positions. The apparent demetalation rate constant of demetalation is denoted as k' in this article, and the k' is followed by an equation, $k' = k[H^+]^n$. Figure 3 depicts kinetic plots of the Soret absorbance of four Chl *a* analogs as well as Chl *a* in acetone/water (3/1, vol/vol) at the proton concentration of 1.2×10^{-3} M. Their demetalation reactions were regarded as pseudo-first-order reactions because of linear time-dependency of the logarithm of Soret absorbance in their reactions. This is consistent with the reaction conditions in which the proton concentration was much higher than the concentration of the Chl *a* analogs. Such pseudo-first-order demetalation kinetics was also observed at the lower proton concentrations of 2.5×10^{-4} and 1.2×10^{-4} M. Therefore, apparent reaction rate constants of the demetalation, k's, could be estimated by fitting the time courses of the Soret absorbance of the Chl *a* analogs to the following kinetic equation:

$$\ln(A - A_\infty)/(A_0 - A_\infty) = -k't$$

where A_0, A and A_∞ are their Soret absorbance at the onset of the measurement, at time t, and at the complete demetalation, respectively. The k'-values of the four Chl *a* analogs are summarized in Fig. 4, and are compared with those of Chl *a*. The k's in Fig. 4 are the averages of more than three independent measurements; their standard deviations were less than 6, 11, 12, 5 and 4% of the averages of the k's for DV-Chl *a*, mesoChl *a*, pyroChl *a*, PChl *a* and Chl *a*, respectively. The logarithm of apparent demetalation rate constants, log k', of all the Chl *a* analogs linearly increased with that of proton concentrations, log $[H^+]$. The slopes of log k' plots against log $[H^+]$ in Fig. 4 were determined to be 1.9, 2.1, 2.0, 2.2 and 1.9 for DV-Chl *a*, mesoChl *a*, pyroChl *a*, PChl *a* and Chl *a*, respectively. The relationships between log k' and log $[H^+]$ allow us to estimate the number of protons that participate in the rate-limiting step of the demetalation reactions, as the k's are followed by the equation, $k' = k[H^+]^n$, where n denotes the proton number involved in the rate-limiting step (26–28). The present results indicate the participation of two protons in the rate-limiting step of removal of the central magnesium from Chl *a* analogs under the acidic conditions. This is consistent with previous works, which mentioned that the proton number in the rate-limiting steps of demetalation of Chl *a*/*a'*, BChl *a*, Zn-Chl *a* and Zn-BChl *a* was *ca* 2 (26–28). These suggest that the rate-limiting step of (B)Chl demetalation is the attack of two protons on two nitrogen atoms in the cyclic tetrapyrroles under acidic conditions.

Effects of 3- and 8-vinyl groups on demetalation

Comparison of apparent demetalation rate constants, k's, among DV-Chl *a*, mesoChl *a* and Chl *a* enables us to unravel the effects of the 3- and 8-vinyl groups on demetalation properties of Chl *a* analogs. The k'-values of DV-Chl *a* were smaller than those of Chl *a* in the proton concentration range between 1.2×10^{-3} and 1.2×10^{-4} M. In contrast, the k's of mesoChl *a* were larger than those of Chl *a* under the acidic conditions. These reveal that the substitution of the ethyl with vinyl group(s) in the A- and/or B-ring(s) of Chl *a* analogs provides the resistance to demetalation under the acidic conditions. The relative ratios of k's of DV-Chl *a* to Chl *a*, k'(DV-Chl *a*)/k'(Chl *a*), were 0.39, 0.42 and 0.45 at the proton concentrations of 1.2×10^{-3}, 2.5×10^{-4} and 1.2×10^{-4} M, respectively, and k'(Chl *a*)/k'(mesoChl *a*) were estimated to be 0.45, 0.53 and 0.63. The former values were slightly

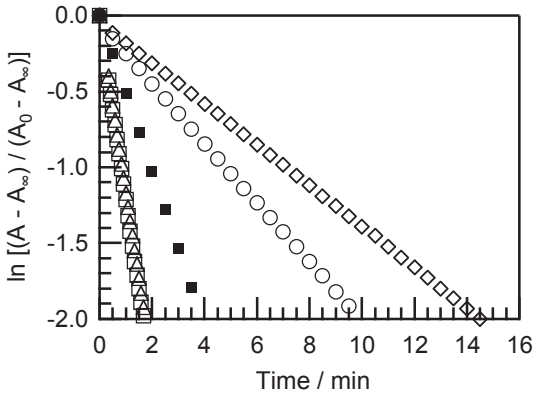

Figure 3. Kinetic plots for demetalation of DV-Chl *a* (open circle), mesoChl *a* (open square), pyroChl *a* (open triangle), PChl *a* (open diamond) and Chl *a* (closed square) in acetone/water (3/1, vol/vol) at the proton concentration of 1.2×10^{-3} M. Absorbance changes were monitored at 440, 427, 433, 435 and 431 nm for DV-Chl *a*, mesoChl *a*, pyroChl *a*, PChl *a* and Chl *a* respectively. A_0, A and A_∞ are Soret absorbance of Chl *a* analogs at the onset of measurements, at time *t*, and at the complete demetalation, respectively.

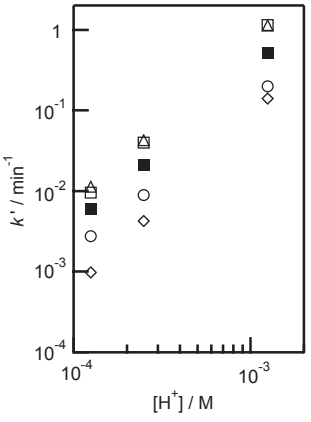

Figure 4. Demetalation rate constants, *k*′s, of DV-Chl *a* (open circle), mesoChl *a* (open square), pyroChl *a* (open triangle), PChl *a* (open diamond) and Chl *a* (closed square) in acetone/water (3/1, vol/vol) dependent on the examined proton concentrations $[H^+]$.

smaller than those of the latter. Such a slight difference might be ascribable to inherent differences of the vinyl groups conjugated to the A- and B-rings.

It has been reported that electron-withdrawing groups such as formyl and acetyl groups directly conjugated with the π-system of cyclic tetrapyrroles slow down removal of the central metal (31,33,34). Such peripheral electron-withdrawing groups would decrease the electron densities of the core nitrogen atoms, preventing electrophilic attack of protons to pyrrole nitrogen atoms. As vinyl group is more electronegative than an ethyl group (41), the vinyl group(s) at the 3- and/or 8-position(s) of Chl *a* analogs also resulted in slower demetalation kinetics. These effects are in line with the previous report, in which zinc 3-vinyl-Chl derivative exhibited slower removal of the central zinc than the corresponding zinc 3-ethyl-chlorin (34).

The substitution effect of weakly electron-withdrawing 8-vinyl group on demetalation properties of Chls is much smaller than the strongly electron-withdrawing 7-formyl effects based on the comparison of the present *k*′-value of DV-Chl *a* with the reported one of Chl *b* under the identical acidic conditions (31). Such a difference between the 8-vinyl and 7-formyl groups would allow DV-Phe *a* to function as the primary electron acceptor in PS II by *in vivo* demetalation of DV-Chl *a* in oxygenic photosynthetic organisms. Further studies will be required to unravel the formation and selection mechanisms of the primary electron accepting Phe molecules in PS II.

Effects of 13^2-methoxycarbonyl group on demetalation

The apparent demetalation rate constants, *k*′s, of pyroChl *a* were compared with those of Chl *a* to examine the effect of the 13^2-methoxycarbonyl group on demetalation of Chl *a*. The *k*′-values of pyroChl *a* were about twice larger than those of Chl *a* in the proton concentration range between 1.2×10^{-3} and 1.2×10^{-4} M, indicating that the 13^2-methoxycarbonyl group in Chl *a* was one of the structural factors to slow down demetalation kinetics. This study first revealed the effect of the 13^2-methoxycarbonyl group in Chl *a* on demetalation properties without other structural effects, although the effect of the stereochemistry at the 13^2-position in Chl *a* was already reported by comparing Chl *a* with its epimer Chl *a*′ (26,27). Mazaki and Watanabe reported 1.4-times faster demetalation kinetics of Chl *a*′ relative to Chl *a* in acidic aqueous acetone, and explained the difference by invoking larger steric repulsion between the 13^2-methoxycarbonyl group and the 17-propionate residue possessing the phytyl ester in Chl *a*′ (26,27). In contrast, faster demetalation kinetics of pyroChl *a* would mainly originate from electronic effects in the isocyclic E-ring rather than steric effects in the case of Chl *a*′. The E-ring of Chl *a* possesses a β-ketoester system, whereas that of pyroChl *a* is a cyclopentanone. This study suggests that the difference in the E-ring would influence electronic states in the chlorin π-macrocycle, especially pyrrole nitrogen atoms, resulting in the difference of demetalation properties between Chl *a* and pyroChl *a*. Homoconjugation of the electron-withdrawing 13^2-methoxycarbonyl group with the 13-keto group ($C13^1$–$C13^2$–CO-OCH_3) and chlorin π-system (C15–$C13^2$–$COOCH_3$) in Chl *a* would decrease the *k*′-values as expected (vide supra). It is noted that the cross-talk effects between the 13^2-methoxycarbonyl group and the C17–C18 double bond might be taken into consideration to understand structure-dependent demetalation properties more precisely.

Effects of macrocycles on demetalation

The apparent demetalation rate constants, *k*′s, of PChl *a*, whose macrocyclic structure was the porphyrin skeleton, were four to six times slower than those of Chl *a* under the acidic conditions. The slow demetalation kinetics of PChl *a* relative to Chl *a* can be ascribed to the porphyrin-type tetrapyrroles, as PChl *a* possessed the same structure as Chl *a* except the bond between C17 and C18 atoms. The effect of the porphyrin skeleton on demetalation kinetics was in line with previous reports (32,35), in which zinc complexes of methyl protopyropheophorbides (porphyrin-type complexes) also exhibited slower demetalation kinetics than the corresponding zinc methyl pyropheophorbides (chlorin-type complexes). These indicate that the porphyrin macrocycle is responsible for resistance to demetalation of PChl-type cyclic tetrapyrroles due to the electronic states and/or flexibility of π-macrocycles.

PChl *a* is an esterified pigment of PChlide *a*, which is an important biosynthetic intermediate and sometimes a photosynthetically

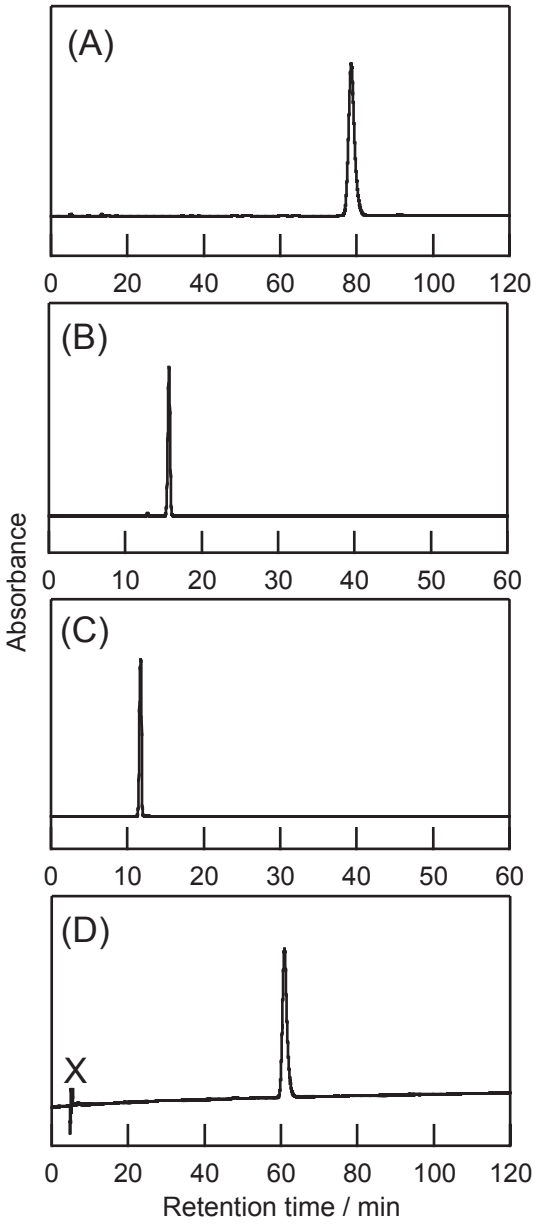

Figure 5. HPLC elution patterns of demetalation products of DV-Chl *a* (A), mesoChl *a* (B), pyroChl *a* (C) and PChl *a* (D) under the conditions in Fig. 3 for 100, 20, 30 and 90 min, respectively. Reaction products of DV-Chl *a* (A) and PChl *a* (D) were eluted on a reverse-phase column $5C_{18}$-AR-II (6 mmφ × 250 mm) with a guard column $5C_{18}$-AR-II (4.6 mmφ × 10 mm) with methanol/acetone (85/15, vol/vol) at a flow rate of 1.0 mL min^{-1}. Reaction products of mesoChl *a* (B) and pyroChl *a* (C) were eluted on a normal-phase column 5SL-II (6 mmφ × 250 mm) with hexane/2-propanol (99/1, vol/vol) at a flow rate of 1.0 mL min^{-1}. Chromatograms (A–D) were recorded at 417, 405, 411 and 418 nm, respectively. The signal denoted by × in the chromatogram (D) was due to direct injection of the reaction mixture.

active pigment in photosynthetic organisms. Demetalation properties of PChl *a*, therefore, are useful for understanding the *in vivo* states of PChlide *a* by invoking the effect of an esterifying phytyl chain. Comparison of demetalation kinetics among Chl *a*, Chlide *a*, Chlide *a* methyl ester and Chlide *a* ethyl ester suggested that the effects of esterifying chains on demetalation properties of chlorophyllous pigments were slight (23). This is in line with no conjugation of an esterifying chain with the chlorin π-macrocycle. Thus, the present results suggest that PChlide *a* has more tolerance to demetalation than Chl *a* and Chlide *a*.

HPLC analysis of reaction products

Reaction products of four Chl *a* analogs under the same acidic conditions as shown in Fig. 3 were analyzed by reverse-phase or normal-phase HPLC as shown in Fig. 5. The products of DV-Chl *a* after reaction under this condition for 100 min exhibited the main fraction at 79 min (Fig. 5A). This fraction had the Soret and Q_y bands at 417 and 666 nm, respectively, in the HPLC eluent, and was ascribed to DV-Phe *a*. In addition, slight fractions due to by-products during the demetalation reaction were detected at 5 and 13 min in this chromatogram. These by-products could not be assigned because of their small amounts. By incubating mesoChl *a* in the acidic aqueous acetone for 20 min, the main fraction was eluted at 16 min, which exhibited the Soret and Q_y bands at 405 and 658 nm, and few fractions except a slight fraction at 13 min were observed (Fig. 5B). The main product at 16 min was ascribable to mesoPhe *a*, and the slight fraction at 13 min would be ascribable to the 13^2-stereoisomer of mesoPhe *a*, mesoPhe *a*′. As the product of pyroChl *a* after 30-min demetalation reaction, sole pyroPhe *a* was detected at 12 min, and no by-product was formed during the reaction (Fig. 5C). In the case of demetalation reaction of PChl *a* for 90 min, the demetalation product of PChl *a*, namely PPhe *a*, which was eluted at 61 min, was predominantly formed (Fig. 5D). A slight fraction at 5 min was produced by side reactions during the reaction process. These HPLC analyses revealed predominant conversion of Chl *a* analogs to the corresponding demetalated pigments (Phes) with few side reactions under the present conditions.

CONCLUSIONS

This study demonstrated structure-dependence on demetalation properties of Chl *a* analogs under weakly acidic conditions. The vinyl group directly conjugated with the chlorin π-system in the A- and/or B-ring(s) of Chl *a* analogs was responsible for slower demetalation kinetics than the ethyl group. The substitution effect was derived from the larger electron-withdrawing ability of a vinyl group than that of an ethyl group. Removal of the methoxycarbonyl group at the 13^2-position in Chl *a* resulted in faster demetalation kinetics, which was also ascribed to its electron-withdrawing moiety through homconjugation. The porphyrin-type macrocycle of PChl *a* provided the resistance to demetalation. These physicochemical properties on demetalation of Chl *a* analogs will be a clue to solving an enigma concerning *in vivo* Chl demetalation such as production of the primary electron acceptors in PS II reaction centers and the early processes in the Chl *a* degradation.

Acknowledgements—We thank Dr. Yuichiro Kashiyama, Dr. Taichi Yoshitomi, Ms. Yuki Kimura, Mr. Daisuke Takekoshi, and Ms. Haruna Yokota of Ritsumeikan University for their assistance in the preparation of chlorophyllous pigments. This work was partially supported by Grants-in-Aid for Scientific Research (C) (no. 23550201) (to YS) and (A) (no. 22245030) (to HT) from the Japan Society for the Promotion of Science.

REFERENCES

1. Scheer, H. (2006) An overview of chlorophylls and bacteriochlorophylls: biochemistry, biophysics, functions and applications. In

Chlorophylls and Bacteriochlorophylls: Biochemistry, Biophysics, Functions and Applications (Edited by B. Grimm, R. J. Porra, W. Rüdiger and H. Scheer), pp. 1–26. Springer, Dordrecht.
2. Tamiaki, H. and M. Kunieda (2011) Photochemistry of chlorophylls and their synthetic analogs. In *Handbook of Porphyrin Science*, Vol. 11 (Edited by K. M. Kadish, K. M. Smith and R. Guilard), pp. 223–290. World Scientific, Singapore.
3. Chisholm, S. W., R. J. Olson, E. R. Zettler, R. Goericke, J. B. Waterbury and N. A. Welschmeyer (1988) A novel free-living prochlorophyte abundant in the oceanic euphotic zone. *Nature* **334**, 340–343.
4. Chisholm, S. W., S. L. Frankel, R. Goericke, R. J. Olson, B. Palenik, J. B. Waterbury, L. West-Johnsrud and E. R. Zettler (1992) *Prochlorococcus marinus* nov. gen. nov. sp.: An oxygenic marine prokaryote containing divinyl chlorophyll *a* and *b*. *Arch. Microbiol.* **157**, 297–300.
5. Goericke, R. and D. J. Repeta (1992) The pigments of *Prochlorococcus marinus*: The presence of divinyl chlorophyll *a* and *b* in a marine prokaryote. *Limnol. Oceanogr.* **37**, 425–433.
6. Miyashita, H., H. Ikemoto, N. Kurano, K. Adachi, M. Chihara and S. Miyachi (1996) Chlorophyll *d* as a major pigment. *Nature* **383**, 402.
7. Murakami, A., H. Miyashita, M. Iseki, K. Adachi and M. Mimuro (2004) Chlorophyll *d* in an epiphytic cyanobacterium of red algae. *Science* **303**, 1633.
8. Klimov, V. V., A. V. Klevanik, V. A. Shuvalov and A. A. Krasnovsky (1977) Reduction of pheophytin in the primary light reaction of photosystem II. *FEBS Lett.* **82**, 183–186.
9. Klimov, V. V., V. A. Shuvalov and U. Heber (1985) Photoreduction of pheophytin as a result of electron donation from the water-splitting system to Photosystem II reaction centers. *Biochim. Biophys. Acta* **809**, 345–350.
10. Hastings, G., J. R. Durrant, J. Barber, G. Porter and D. R. Klug (1992) Observation of pheophytin reduction in photosystem two reaction centers using femtosecond transient absorption spectroscopy. *Biochemistry* **31**, 7638–7647.
11. Loll, B., J. Kern, W. Saenger, A. Zouni and J. Biesiadka (2005) Towards complete cofactor arrangement in the 3.0 Å resolution structure of photosystem II. *Nature* **438**, 1040–1044.
12. Ohashi, S., T. Iemura, M. R. Islam, Y. Kuroiwa, Y. Kato, M. Ohnishi-Kameyama, T. Watanabe, H. Koike and M. Kobayashi (2009) Divinyl-chlorophyll *a′* and divinyl-pheophytin *a* as key components in a slr1923-inactivated mutant of *Synechocystis* 6803. *Phycologia* **48**, 98.
13. Benz, J. and W. Rüdiger (1981) Chlorophyll biosynthesis: Various chlorophyllides as exogenous substrates for chlorophyll synthase. *Z. Naturforsch.* **36c**, 51–57.
14. Rüdiger, W. (2000) The last steps of chlorophyll synthesis. In *Porphyrin Handbook*, Vol. 13 (Edited by K. M. Kadish, K. M. Smith and R. Guilard), pp. 71–108. Academic Press, San Diego.
15. Kräutler, B. and P. Matile (1999) Solving the riddle of chlorophyll breakdown. *Acc. Chem. Res.* **32**, 35–43.
16. Hörtensteiner, S. (2006) Chlorophyll degradation during senescence. *Annu. Rev. Plant Biol.* **57**, 55–77.
17. Kräutler, B. (2008) Chlorophyll breakdown and chlorophyll catabolites in leaves and fruit. *Photochem. Photobiol. Sci.* **7**, 1114–1120.
18. Hörtensteiner, S. and B. Kräutler (2011) Chlorophyll breakdown in higher plants. *Biochim. Biophys. Acta* **1807**, 977–988.
19. Schelbert, S., S. Aubry, B. Burla, B. Agne, F. Kessler, K. Krupinska and S. Hörtensteiner (2009) Pheophytin pheophorbide hydrolase (pheophytinase) is involved in chlorophyll breakdown during leaf senescence in *Arabidopsis*. *Plant Cell* **21**, 767–785.
20. Büchert, A. M., P. M. Civello and G. A. Martínez (2011) Chlorophyllase versus pheophytinase as candidates for chlorophyll dephytilation during senescence of broccoli. *J. Plant Physiol.* **168**, 337–343.
21. Mackinney, G. and M. A. Joslyn (1940) The conversion of chlorophyll to pheophytin. *J. Am. Chem. Soc.* **62**, 231–232.
22. Mackinney, G. and M. A. Joslyn (1941) Chlorophyll-pheophytin: Temperature coefficient of the rate of pheophytin formation. *J. Am. Chem. Soc.* **63**, 2530–2531.
23. Schanderl, S. H., C. O. Chichester and G. L. Marsh (1962) Degradation of chlorophyll and several derivatives in acid solution. *J. Org. Chem.* **27**, 3865–3868.
24. Rosoff, M. and C. Aron (1965) Reaction kinetics of monomolecular films of chlorophyll *a* on aqueous substrates. *J. Phys. Chem.* **69**, 21–24.
25. Berezin, B. D., A. N. Drobysheva and L. P. Karmanova (1976) Kinetics and mechanism of the dissociation of chlorophyll and its metalloanalogues in proton-donating media. *Russ. J. Phys. Chem.* **50**, 720–723.
26. Mazaki, H. and T. Watanabe (1988) Pheophytinization of chlorophyll *a* and chlorophyll *a′* in aqueous acetone. *Bull. Chem. Soc. Jpn.* **61**, 2969–2970.
27. Mazaki, H., T. Watanabe, T. Takahashi, A. Struck and H. Scheer (1992) Pheophytinization of eight chlorophyll derivatives in aqueous acetone. *Bull. Chem. Soc. Jpn.* **65**, 3212–3214.
28. Kobayashi, M., M. Yamamura, M. Akiyama, H. Kise, K. Inoue, M. Hara, N. Wakao, K. Yahara and T. Watanabe (1998) Acid resistance of Zn-bacteriochlorophyll *a* from an acidophilic bacterium *Acidiphilum rubrum*. *Anal. Sci.* **14**, 1149–1152.
29. Saga, Y., Y. Hirai and H. Tamiaki (2007) Kinetic analysis of demetalation of bacteriochlorophyll *c* and *e* homologs purified from green sulfur photosynthetic bacteria. *FEBS Lett.* **581**, 1847–1850.
30. Hirai, Y., H. Tamiaki, S. Kashimura and Y. Saga (2009) Physicochemical studies of demetalation of light-harvesting bacteriochlorophyll isomers purified from green sulfur photosynthetic bacteria. *Photochem. Photobiol.* **85**, 1140–1146.
31. Hirai, Y., H. Tamiaki, S. Kashimura and Y. Saga (2009) Demetalation kinetics of natural chlorophylls purified from oxygenic photosynthetic organisms: Effect of the formyl groups conjugated directly to the chlorin π-macrocycle. *Photochem. Photobiol. Sci.* **8**, 1701–1707.
32. Saga, Y., S. Hojo and Y. Hirai (2010) Comparison of demetalation properties between zinc chlorin and zinc porphyrin derivatives: Effect of macrocyclic structures. *Bioorg. Med. Chem.* **10**, 5697–5700.
33. Hirai, Y., S. Kashimura and Y. Saga (2011) Demetalation kinetics of chlorophyll derivatives possessing different substituents at the 7-position under acidic conditions. *Photochem. Photobiol.* **87**, 302–307.
34. Hirai, Y., S. Sasaki, H. Tamiaki, S. Kashimura and Y. Saga (2011) Substitution effects in the A- and B-rings of the chlorin macrocycle on demetalation properties of zinc chlorophyll derivatives. *J. Phys. Chem. B* **115**, 3240–3244.
35. Saga, Y., R. Miura, K. Sadaoka and Y. Hirai (2011) Kinetic analysis of demetalation of synthetic zinc cyclic tetrapyrroles possessing an acetyl group at the 3-position: effects of tetrapyrrole structures and peripheral substitution. *J. Phys. Chem. B* **115**, 11757–11762.
36. Wakao, N., N. Yokoi, N. Isoyama, A. Hiraishi, K. Shimada, M. Kobayashi, H. Kise, M. Iwaki, S. Itoh, S. Takaichi and Y. Sakurai (1996) Discovery of natural photosynthesis using Zn-containing bacteriochlorophyll in aerobic bacterium *Acidiphilium rubrum*. *Plant Cell Physiol.* **37**, 889–893.
37. Kobayashi, M., M. Akiyama, H. Kise and T. Watanabe (2006) Unusual tetrapyrrole pigments of photosynthetic antenna and reaction centers: specially-tailored chlorophylls. In *Chlorophylls and Bacteriochlorophylls: Biochemistry, Biophysics, Functions and Applications* (Edited by B. Grimm, R. J. Porra, W. Rüdiger and H. Scheer), pp. 55–66. Springer, Dordrecht.
38. Mizoguchi, T., C. Nagai, M. Kunieda, Y. Kimura, A. Okamura and H. Tamiaki (2009) Stereochemical determination of the unique acrylate moiety at the 17-position in chlorophylls-*c* from a diatom *Chaetoseros calcitrans* and its effect upon electronic absorption properties. *Org. Biomol. Chem.* **7**, 2120–2126.
39. Tamiaki, H., D. Takekoshi and T. Mizoguchi (2011) Reduction of vinyl groups in naturally occurring chlorophylls-*a*. *Bioorg. Med. Chem.* **19**, 52–57.
40. Mizoguchi, T., A. Shoji, M. Kunieda, H. Miyashita, T. Tsuchiya, M. Mimuro and H. Tamiaki (2006) Stereochemical determination of chlorophyll-*d* molecule from *Acaryochloris marina* and its modification to a self-aggregative chlorophyll as a model of green photosynthetic bacterial antennae. *Photochem. Photobiol. Sci.* **5**, 291–299.
41. Inamoto, N. and S. Masuda (1982) Revised method for calculation of group electronegativities. *Chem. Lett.* **7**, 1003–1006.

Copyright of Photochemistry & Photobiology is the property of Wiley-Blackwell and its content may not be copied or emailed to multiple sites or posted to a listserv without the copyright holder's express written permission. However, users may print, download, or email articles for individual use.